



ISSN ONLINE: 2447-0228

## ITEGAM-JETIA

Manaus, v.9 n.40, p. 39-50. Mar/Apr, 2023.  
DOI: <https://doi.org/10.5935/jetia.v9i40.857>









RESEARCH ARTICLE

OPEN ACCESS

## DESIGN AND CONSTRUCTION OF A FUZZY LOGIC SOLAR TRACKER PROTOTYPE FOR THE OPTIMIZATION OF A PHOTOVOLTAIC SYSTEM

Omar Beltrán González<sup>1</sup>, Jesús Hernández Aguilar<sup>2</sup>, Francisco Eneldo López Monteagudo<sup>\*3</sup>, Rafael Villela Varela<sup>4</sup>, Aurelio Beltrán Telles<sup>5</sup> and Claudia Reyes Rivas<sup>6</sup>

<sup>1, 2, 3, 4, 5, 6</sup> Autonomous University of Zacatecas, Av. López Velarde No. 801 CP 98060 Zacatecas, México.

<sup>1</sup> <http://orcid.org/0009-0006-6647-7014> , <sup>2</sup> <http://orcid.org/0009-0000-6461-0762> , <sup>3</sup> <http://orcid.org/0000-0001-6082-1546> ,  
<sup>4</sup> <http://orcid.org/0000-0003-0088-4718> , <sup>5</sup> <http://orcid.org/0000-0001-8757-2041> , <sup>6</sup> <http://orcid.org/0000-0001-9028-2096> 

Email: [omar@uaz.edu.mx](mailto:omar@uaz.edu.mx), [jesush@uaz.edu.mx](mailto:jesush@uaz.edu.mx), [\\*eneldolm@yahoo.com](mailto:*eneldolm@yahoo.com), [wrvrmx@yahoo.com.mx](mailto:wrvrmx@yahoo.com.mx), [abeltral@uaz.edu.mx](mailto:abeltral@uaz.edu.mx), [clausy\\_17@yahoo.com](mailto:clausy_17@yahoo.com)

### ARTICLE INFO

#### Article History

Received: March 29<sup>th</sup>, 2023

Accepted: April 26<sup>th</sup>, 2023

Published: April 29<sup>th</sup>, 2023

#### Keywords:

Photovoltaic panels,  
Solar energy,  
Solar tracker.

### ABSTRACT

In this article, a fuzzy logic solar tracker was designed and implemented to increase the efficiency of a photovoltaic system by updating the position of the panel throughout the day for optimal use of solar radiation. In the design and implementation of the solar tracker, different control strategies were analyzed, concluding that the fuzzy control satisfies all the requirements of the photovoltaic system with a solar tracker, the developed prototype underwent different tests in a determined period of time to validate the performance of the solar tracker. system compared to one with a fixed position, achieving an increase of 40% compared to fixed solar systems.



Copyright ©2023 by authors and Galileo Institute of Technology and Education of the Amazon (ITEGAM). This work is licensed under the Creative Commons Attribution International License (CC BY 4.0).

## I. INTRODUCTION

At present, the predominant energy medium is from fossil fuels, which is being diminished due to industrial growth, means of transportation and population, increasing demand for it, to meet this increase in demand. demand the most viable alternative is renewable energy. Within these renewable energies, solar energy is the most viable because it is a resource that occurs anywhere, it does not depend on its geographical location, unlike other alternative energies [1].

Photovoltaic solar energy is that which is obtained through the direct transformation of the sun's energy into electrical energy through solar cells [2].

Solar energy is one of the most viable alternative sources since it is present throughout the planet, the energy from the sun is inexhaustible and contributes to reducing current environmental problems that have been a consequence of the irrational use of fuels. fossils [3].

The energy produced by solar panels depends directly on the position of the sun with respect to said panel. The constant change of position of the sun considerably limits the efficiency of a panel in a fixed state, therefore, through the use of solar trackers,

it is sought to make the most of the irradiation of the sun's rays, increasing the power level. electricity generated in the photovoltaic system compared to fixed systems [4].

The photoelectric cells transform solar energy into electricity in the form of direct current and this is transformed into alternating current by means of an inverter to guarantee the parameters of the electrical network in interconnected systems, so that the converter works in the zone of maximum efficiency solar trackers are used [5].

In photovoltaic systems connected to the electrical grid, the inverter is the central core and must have certain protections in situations that may occur in the electrical grid, such as voltage out of range, grid outage, grid phase shift. [6].

Solar trackers, depending on the type of movement, can be one-axis or two-axis [7].

In single-axis solar trackers, the solar panels remain approximately perpendicular to the sun's rays, following the sun from east to west, with a minimum degree of complexity and lower cost compared to other types of trackers. The limitation of this type of tracker is that it cannot fully track the sun, since it can only track the azimuth or the solar inclination, but not both [8].

Two axis solar trackers have two degrees of freedom and are capable of fully tracking the sun, both in inclination and azimuth, although the performance of the installation may be superior compared to single-axis ones, their cost is much higher [9].

The tracker described in this article belongs to the classification of trackers of an azimuthal axis whereby the panels remain approximately perpendicular to the sun's rays, following the sun from sunrise to sunset.

## II. METHODOLOGY

The objective of this article was to design and implement a control system that allows the photovoltaic system to follow the path of the sun to improve the efficiency in the generation of electrical energy compared to fixed systems.

Fuzzy logic has played a vital role in advancing practical solutions for a wide variety of applications in automatic control engineering, digital signal processing, communications, expert systems, medicine, etc. However, the most significant applications of fuzzy systems have been concentrated specifically in the area of automatic control.

Different studies applied to fuzzy control theory have shown that fuzzy learning and/or fuzzy control algorithms are one of the most active and fruitful areas of research in recent years within the field of fuzzy logic [10].

### II.1 ESTRUCTURA DE LOS SISTEMAS DIFUSOS

The Different studies applied to fuzzy control theory have shown that fuzzy learning and/or fuzzy control algorithms are one of the most active and fruitful areas of research in recent years within the field of fuzzy logic.

From the conceptual point of view, the design of fuzzy systems from input-output pairs have been classified into two types. The first type of classification suggests that the rules are generated through the input-output pairs and the structure of the fuzzy system is built from these rules, from the fuzzy inference mechanism of the fuzzifier and the defuzzifier. In the second classification, the structure of the fuzzy system is specified first so that some parameters in the fuzzy structure are free to change and these are determined according to the input-output pairs. Although regularly some applications of fuzzy control to industrial processes have produced results superior to their equivalents obtained by classical control, the domain of these applications has experienced a serious limitation when expanding it to more complex systems, due to the fact that There is not yet a complete theory to determine the performance of the systems from the change in its parameters or variables.

Fuzzy inference systems have currently found several successful applications within a wide variety of areas such as automatic control, data classification, decision analysis, expert systems, time series prediction, etc. robotics and pattern recognition. Because of their multidisciplinary nature, fuzzy inference systems are known as expert systems, fuzzy models, fuzzy logic controllers, or just fuzzy systems.

Essentially a fuzzy system, it is a structure based on knowledge defined through a set of fuzzy rules, which contain a fuzzy logical quantification of the expert's linguistic description of how to perform adequate control. Figure 1 illustrates the block diagram and the basic components of a fuzzy system where the classical sets  $U_i$  and  $Y_i$  are called the universe of discourse for  $u_i$  and  $y_i$  respectively. In particular,  $u_i \in U_i$  with  $i = 1, 2, 3, \dots, n$  and

$y_i \in Y_i$  with  $i = 1, 2, \dots, m$ , where  $u_i$  and  $y_i$  correspond to the inputs and outputs of the fuzzy system.

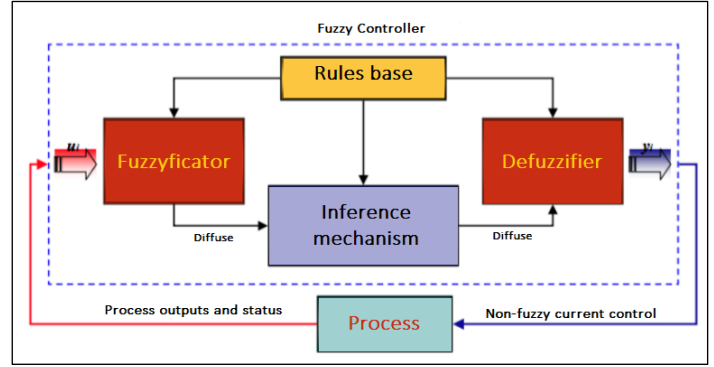


Figure 1: General scheme of fuzzy control.

Source: [12].

In figure 1, it can be seen that the fuzzy system uses fuzzy sets, defined by the fuzzy rule base, to quantify the information in the rule base and that the inference mechanism operates on these fuzzy sets to produce new sets. Therefore, it is necessary to specify how the system will convert the numerical inputs  $u_i \in U_i$  into fuzzy sets, a process called "fuzzification", such that they can be used by the fuzzy system. Similarly, the process called defuzzification describes the mapping of a space of fuzzy control actions into non-fuzzy control actions. Defuzzification therefore generates a non-fuzzy control action which we generally denote by  $y_i$  and is the best representation of an inferred fuzzy output.

The fuzzification process consists of a transformation of a datum from a classical set to its corresponding fuzzy set, therefore, we denote by  $U_i^*$ , the set of all possible fuzzy sets that can be defined by  $U_i$  and given  $u_i \in U_i$ , let us denote the fuzzy transformation of  $u_i$  to a fuzzy set by  $A_{ifuz}$ , which is defined in the universe of discourse  $U_i$ . The transformation from a classical set to a fuzzy set is produced by using the fuzzification operator  $F$ , [11], defined by  $F: U_i \rightarrow U_i^*$ , where  $F(u_i) = A_{ifuz}$ . Regularly the use of the singleton type fuzzifier is the most widely used for applications in the area of automatic control and this is defined as a fuzzy set  $A_{ifuz} \in U_i^*$  with membership function.

$$\mu_{A_i}^{fuz}(x) = \begin{cases} 1 & \text{si } x = u_i \\ 0 & \text{en otro caso} \end{cases} \quad (1)$$

Any fuzzy set with the form 1 in its membership function is called "singleton", figure 2.

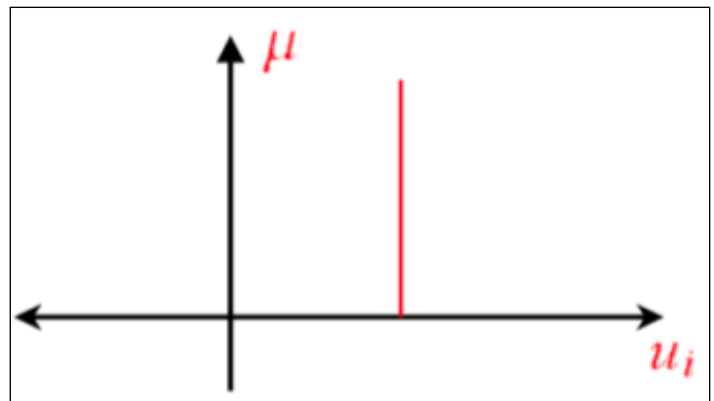


Figure 2: Singleton membership function.

Source: [12].

The first step for the control design is the transformation of the domain so that the values delivered by the sensors are transformed to fuzzy inputs. For each input and output it is required to have an adequate number of labels that adequately describe their behavior. A universe of discourse with more labels is more accurate than one with few labels, however, it will also require more processing time. Also, an excessive number of labels can lead to an unstable fuzzy system.

### II.2 FUZZY INFERENCE MECHANISM

The fuzzy inference mechanism is the core of any fuzzy controller. Its behavior is generally characterized by a set of fuzzy rules of the form:

$$\text{If } x \text{ is } A \text{ then } y \text{ is } B \quad (2)$$

Where A and B are linguistic values defined by a fuzzy set in a universe X and Y respectively. The If clause, an antecedent, is a control action given to the process under control. With a set of fuzzy rules, the fuzzy inference mechanism is capable of deriving a control action for a set of input values, determining a control action for the observed inputs, which represent the state of the process to be controlled. -side by using control rules. The expression "If x is A then y is B," which is regularly abbreviated  $A \rightarrow B$ , is essentially a binary relation R of the variables x and y on the product space  $X \times Y$ . There are several fuzzy inference methods that can be formulated through the t-norm and s-norm operators to calculate the fuzzy relation  $R = A \rightarrow B$ .

### II.3 FUZZY INFERENCE MECHANISM

Defuzzification is defined as a mapping from a fuzzy set B' in  $V \subset R$  (which is the output of fuzzy inference) to an element of a classical set  $yq^{crisp} = y * \in V$ .

Conceptually, the task of defuzzifying is to specify a point, an element of V, that reflects the best representation of the fuzzy set B'. To date there is no optimal algorithm for defuzzification, however, there are different defuzzification techniques that are easy to implement.

There are different fuzzy controllers, the most widely used are Mamdani and Sugeno, which have been used successfully in a wide variety of applications in the fuzzy control community. Although, the objective of the Mamdani fuzzy controller is to represent a successful human operator, the Sugeno-type fuzzy controller is suggested to be more efficient in computational and learning methods.

## III. SOLAR TRACKER CONTROL PLATFORM DESIGN

For the design of the control platform, two degrees of freedom were used, considering an azimuthal axis and a polar axis, allowing the photovoltaic cell system to position itself parallel to the sun's rays, achieving its highest efficiency. regardless of your geographical position or time of day. For the implementation of the controller, an Arduino card was used through which the movement of the two motors is controlled, positioning the platform in its different axes.

The support structure was designed considering the type of movement desired for the solar tracker, the size of the solar panels and the available space.

The control system uses optical sensors, which monitor the variations in light levels emitted by the sun in order to know the position in which it is located. In this way, analog signals are

obtained that will later be converted to digital signals and implemented as variables in a program in charge of feeding the motors to move the structure and position it parallel to the incidence of the sun's rays.

The built mechanical structure is made up of various parts:

1. Structure support
2. Rectangular panel support
3. Concrete base
4. Counterweight
5. DC motors
6. Toothed disk azimuthal movement
7. Worm azimuthal movement
8. Polar movement worm
9. Toothed disc polar movement

In the figure 3 shows the parts of the mechanical structure.



Figure 3: Parts of the structure.  
Source: Authors, (2022).

In the figure 4 shows the parts of the azimuthal axis.

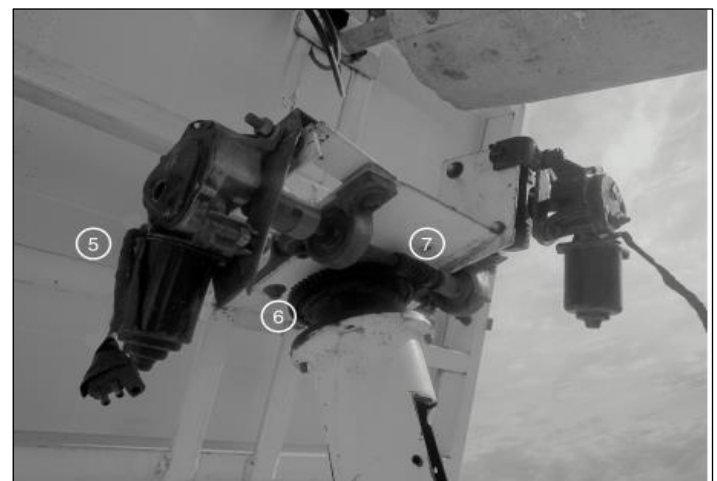


Figure 4: Parts of the azimuthal axis structure.  
Source: Authors, (2022).



In the figure 5 shows the parts of the polar axis.

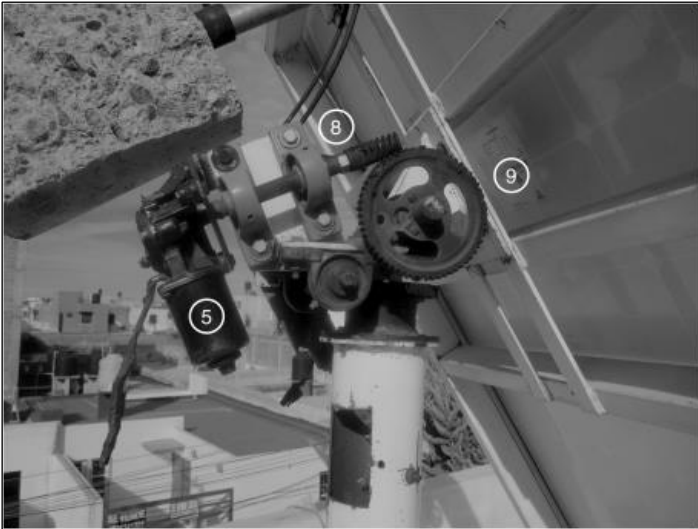


Figure 5: Shows the parts of the azimuthal axis.  
Source: Authors, (2022).

In the figure 6 shows the solar panel used.

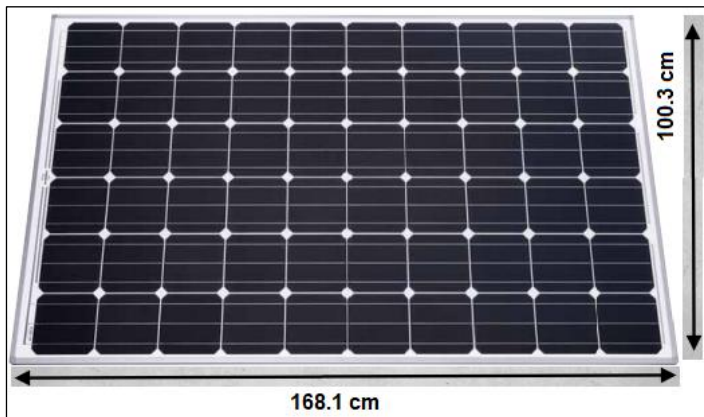


Figure 6: Used solar panel (Produced in Germany).  
Source: Authors, (2022).

In order to monitor the solar movement throughout the day and during the seasons of the year, a circuit was implemented to compare the reading of a pair of photoresistive components (LDR), located parallel to each other on the surface and separated by a perpendicular plate that provides a shadow that makes the readings of said devices vary, generating an inequality unless they are located parallel to the sun, this inequality in the readings of said elements is used to locate the panel in the optimal position. The circuit was located in a translucent container conditioned to avoid the interference of solar rays with incidents not necessary for its application. The circuit shown in figure 5 has an arrangement of L298N, which can handle a voltage of up to 46 Volts, through the two output terminals the direction of rotation of the motor is controlled, the supply voltage for this motor is 17 volts which are obtained from an external source, the control system has three terminals for the direction and speed control signals of the motor to be controlled. If both inputs are low, the motor will be off and there is no power consumption, the speed being controlled by PWM (Pulse Width Modulation). Applying the PWM signal to one of the control inputs of the bridge.

To control the system, an Arduino card supported on a free Hardware platform was used, based on a board with a

microcontroller, which is programmed using its own language and a free integrated development environment (IDE). As it is a free Hardware development platform, both its design and its implementation are free without the need to previously acquire a license.

The developed platform used an Arduino UNO with an ATmega328 microcontroller (data-sheet). It has 14 digital input/output pins (of which 6 of them were used as PWM outputs), 6 analog inputs, a 16MHz crystal oscillator, a USB connection, a power jack, an ICSP header, and a reset button. The microcontroller connects to a computer via USB, is powered by an AC/DC adapter, or a battery. The Arduino Uno Board differs from its predecessor in that it does not require the use of the FTDI USB-to-serial driver chip. Instead, it has the Atmega8U2 programmed as a USB-to-serial converter. ONE.

Atmega328 has 32 KB of flash memory for code storage (of which 0.5 KB is used for the bootloader); it also has 2 KB of SRAM and 1 KB of EEPROM (which can be read and written with the EEPROM library).

Each of the 14 digital pins on the Arduino UNO board can be used as input or output, using the `pinMode()`, `digitalWrite()`, and `digitalRead()` functions. They all operate at 5 volts, each pin can supply or receive a maximum of 40 mA and have an internal pull-up resistor (disconnected by default) of 20-50 K $\Omega$ . In addition, some pins have specialized functions. The configuration of the Arduino UNO used is shown in figure 7.

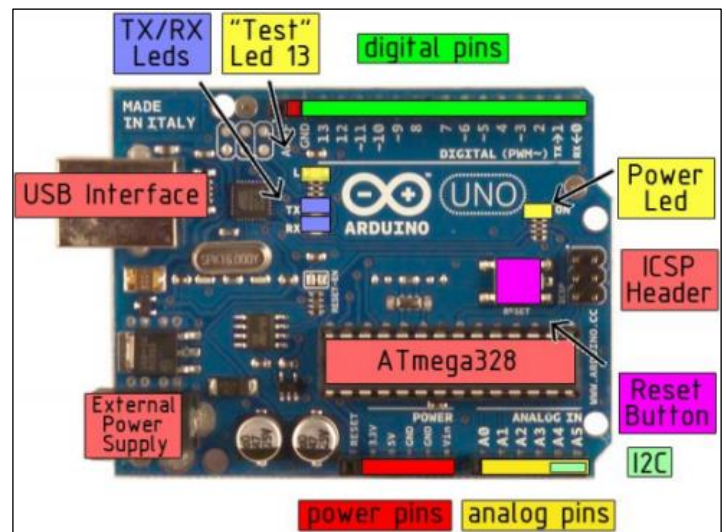


Figure 7: Arduino UNO Configuration.  
Source: [10].

The Hardware of the card used consists of a board with an Atmel AVR microcontroller and input/output ports.

#### IV. PROGRAMMING OF THE MEMBER UNIONS OF THE SOLAR TRACKER

For the elaboration of the control program of the solar tracker, knowing the behavior of the different devices that will make possible the control of the system, the member functions that are used in the programming will be elaborated, to corroborate the correct operation, the Fuzzy Logic Controller Design package from the LabView program, this was only used for the simulation of the control algorithms since Arduino does not have a simulation environment. For each of the input and output variables, the universe of discourse is defined in which the member functions of each of the variables will be contained.

For the fuzzy control, a natural language was used through which the functions of each variable are expressed with a name to distinguish them and use them later.

Table 1: Input variables.

Name	Range	Number of member functions
Photo_l $0 \geq 600$ 4	Photo_l $0 \geq 600$ 4	Photo_l $0 \geq 600$ 4
Photo_r $0 \geq 600$ 4	Photo_r $0 \geq 600$ 4	Photo_r $0 \geq 600$ 4
Pot_A $660 \geq 880$ 3	Pot_A $660 \geq 880$ 3	Pot_A $660 \geq 880$ 3
Pot_G Trapezoide 3	Pot_G Trapezoide 3	Pot_G Trapezoide 3

Source: Authors, (2022).

In the table 2 shows the output variables.

Table 2: Output variables.

Name	Range	Number of member functions
ACCW	$0 \geq 255$	3
ACW	$0 \geq 255$	3
GCW	$0 \geq 255$	3
Pot_G	$0 \geq 255$	3

Source: Authors, (2022).

In the table 3 shows the member functions of Photo l.

Table 3: Photo member functions l.

Membership Function	Shape	Points
DL	Trapezoide	500 ; 525 ; 600 ; 600
DML	Trapezoide	300 ; 400 ; 400 ; 500
ML	Trapezoide	100 ; 200 ; 200 ; 300
BL	Trapezoide	0 ; 0 ; 75 ; 100

Source: Authors, (2022).

Obtaining the graph shown in figure 8 for the member functions of Photo l.

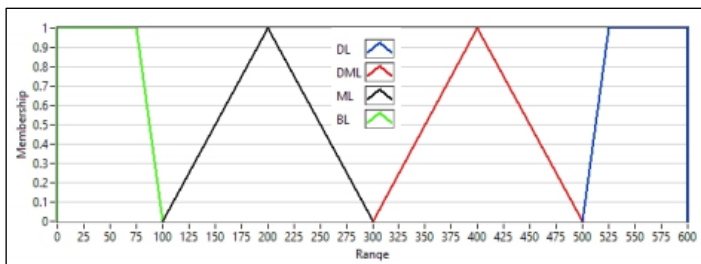


Figure 8: Graph of member functions of Photo l.

Source: Authors, (2022).

In the table 4 shows the member functions of Photo r.

Table 4: Photo member functions r.

Membership Function	Shape	Points
DR	Trapezoide	500 ; 525 ; 600 ; 600
DMR	Trapezoide	300 ; 400 ; 400 ; 500
MR	Trapezoide	100 ; 200 ; 200 ; 300
BR	Trapezoide	0 ; 0 ; 75 ; 100

Source: Authors, (2022).

Obtaining the graph shown in figure 9 for the member functions of Photo r.

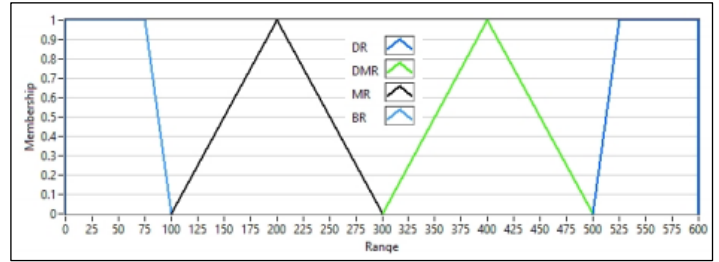


Figure 9: Graph of member functions of Photo r.

Source: Authors, (2022).

In the table 5 shows the member functions of potentiometer A.

Table 5: Member functions of potentiometer A.

Membership Function	Shape	Points
Amin	Trapezoide	660 ; 660 ; 660 ; 700
Asafe	Trapezoide	700 ; 700 ; 840 ; 840
Amax	Trapezoide	840 ; 880 ; 880 ; 880

Source: Authors, (2022).

Obtaining the graph shown in figure 10 for the member functions of potentiometer A.

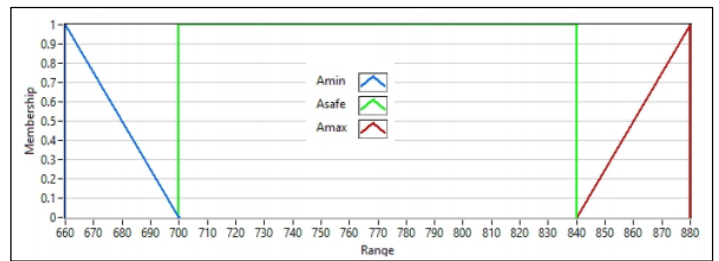


Figure 10: Graph of member functions of Potentiometer A.

Source: Authors, (2022).

In the table 6 shows the member functions of potentiometer G.

Table 6: Member functions of potentiometer G.

Membership Function	Shape	Points
Gmin	Trapezoide	450 ; 450 ; 450 ; 500
Gsafe	Trapezoide	500 ; 500 ; 900 ; 900
Gmax	Trapezoide	900 ; 950 ; 950 ; 950

Source: Authors, (2022).

Obtaining the graph shown in figure 11 for the member functions of potentiometer G.

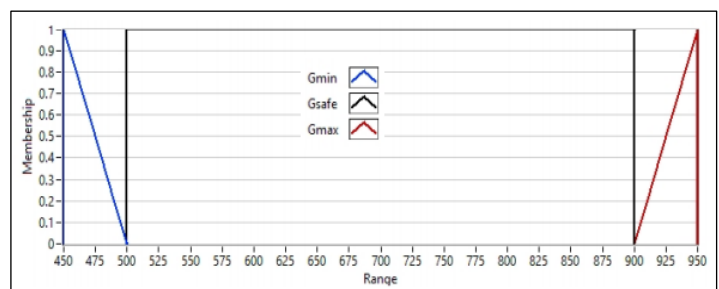


Figure 11: Graph of member functions of Potentiometer G.

Source: Authors, (2022).

In the table 7 shows the member functions of the Polar motion motor.

Table 7: Functions member of the Polar motion motor.

Membership Function	Shape	Points
OFF_ACCW	Trapezoide	0
M_ACCW	Trapezoide	100 ; 140 ; 140 ; 180
ON_ACCW	Trapezoide	180 ; 200 ; 240 ; 255

Source: Authors, (2022).

Obtaining the graph shown in figure 12 for the member functions of the Polar movement motor.

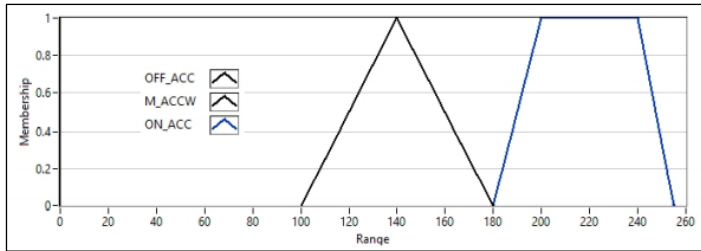


Figure 12: Graph of member functions of the Polar motion motor. Source: Authors, (2022).

In the table 8 shows the member functions of the Polar motion engine.

Table 8: Functions member of the Polar motion engine.

Membership Function	Shape	Points
OFF_ACW	Singleton	0
M_ACW	Trapezoide	100 ; 140 ; 140 ; 180
ON_ACW	Trapezoide	180 ; 200 ; 240 ; 255

Source: Authors, (2022).

Obtaining the graph shown in figure 13 for the member functions of the Polar movement motor.

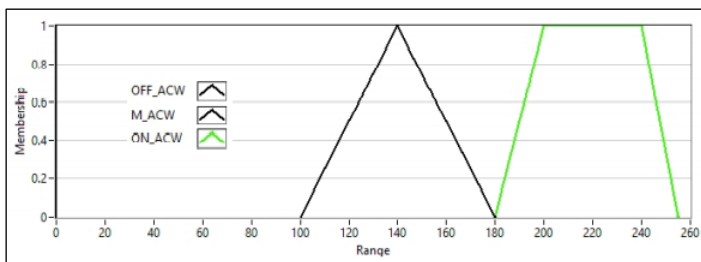


Figure 13: Graph of member functions of the Polar motion motor. Source: Authors, (2022).

In the table 9 shows the member functions of the Azimuthal movement motor.

Table 9: Functions member of the Polar motion motor.

Membership Function	Shape	Points
OFF_GCCW	Singleton	0
M_GCCW	Trapezoide	120 ; 130 ; 170 ; 180
ON_GCCW	Trapezoide	180 ; 200 ; 240 ; 255

Source: Authors, (2022).

Obtaining the graph shown in figure 14 for the member functions of the Azimuthal movement motor.

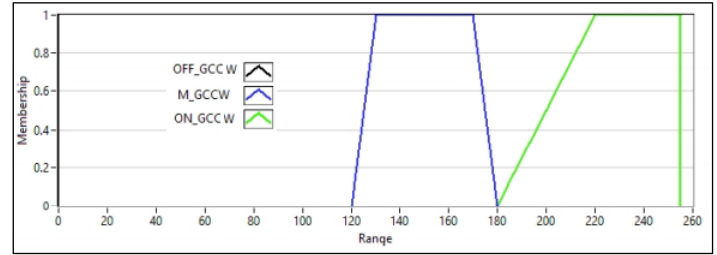


Figure 14: Graph of member functions of the Azimuthal movement motor. Source: Authors, (2022).

In the table 10 shows the member functions of the Azimuthal movement motor.

Table 10: Azimuthal moving engine member functions.

Membership Function	Shape	Points
OFF_GCW	Singleton	0
M_GCW	Trapezoide	120 ; 130 ; 170 ; 180
ON_GCW	Trapezoide	180 ; 220 ; 255 ; 255

Source: Authors, (2022).

Obtaining the graph shown in figure 15 for the member functions of the Azimuthal movement motor.

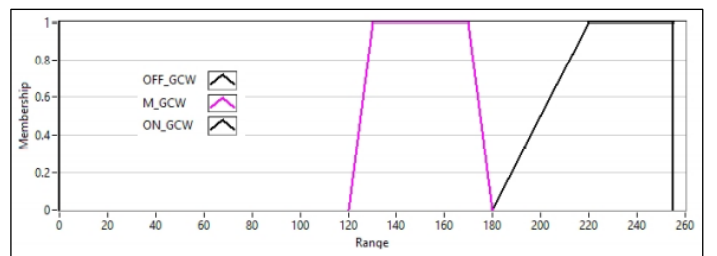


Figure 15: Graph of member functions of the Azimuthal motion motor. Source: Authors, (2022).

## V. RESULTS AND DISCUSSIONS

From the analysis of the data, the hypothesis on the increase in the level of electrical power generated in the photovoltaic system using solar trackers, unlike fixed systems, is corroborated.

In the present research work, a functional fuzzy control system was designed and implemented in a mechanical structure; to which different tests were carried out with satisfactory results. The results were obtained by means of the Arduino card, sensing the photoresistive elements between the values of 0 to 1023, varying the readings in a range of 0 to 600 depending on the incidence of solar rays.

In order to verify the correct operation of the control system of the solar tracker, calibration tests were carried out making a greater amount of light fall on one of the photosensitive elements and checking that the motor rotates in that direction.

To corroborate the objective set out in the investigation "A control system was designed to improve the efficiency for the generation of electrical energy with a solar tracker". Measurements were made to compare the energy generated by a fixed panel and the automated system with the implemented fuzzy control, for which I connect a load made up of five 60-watt spotlights placed in series.

Data acquisition was carried out over three days during the month of November 2020, obtaining a total of 113 samples for each

day; using for this purpose four multimeters connected to the load: two of them used for voltage readings and the other two for current readings in both cases, both in the fixed state and in the mobile state.

A test was carried out with a moving solar panel taking into account only the polar movement of the structure from an initial position of 15o inclination on said axis and facing east for sunrise. The control system designed maintained the orthogonality between the panel and the incidence of the sun's rays in order to obtain the

greatest possible efficiency throughout the course of the day, controlling the position through the use of a card. Arduino through the values delivered by the photoresistors moving it as appropriate.

Voltage and current measurements were carried out between 8:40 a.m. and 5:00 p.m. and 6:00 p.m. and with these readings the power and energy generated by the solar panel were determined.

In the table 11 shows the measurements of the first day between 8:40 a.m. and 5:00 p.m. and 6:00 p.m.

Table 11: Comparative measurements of the first day.

Hour	fixed panel			mobile panel		
	Voltage	Current	Power	Voltage	Current	Power
8:40	29.86	1.065	31.8009	33.1	1.1	36.41
8:45	30.25	1.075	32.5187	33.4	1.11	37.07
8:50	30.69	1.084	33.2679	33.3	1.11	36.96
8:55	30.89	1.067	32.9596	33.2	1.11	36.85
9:00	31.14	1.093	34.0360	33.1	1.11	36.74
9:05	31.44	1.098	34.5211	33.1	1.11	36.74
9:10	31.47	1.098	34.5540	33.2	1.11	36.84
9:15	31.66	1.102	34.8893	33.2	1.11	36.85
9:20	31.9	1.105	35.2495	33.3	1.11	36.95
9:25	32.02	1.108	35.4781	33.3	1.11	36.96
9:30	32.09	1.11	35.6199	33.1	1.11	36.74
9:35	32.09	1.11	35.6199	33	1.11	36.63
9:40	32.19	1.12	36.0528	33	1.11	36.63
9:45	32.27	1.114	35.9487	32.8	1.1	36.08
9:50	32.22	1.113	35.8608	32.8	1.1	36.08
9:55	32.37	1.115	36.0925	32.9	1.1	36.19
10:00	32.19	1.112	35.7952	32.8	1.1	36.08
10:05	32.19	1.113	35.8274	32.8	1.1	36.08
10:10	32.2	1.113	35.8386	32.8	1.1	36.08
10:15	32.13	1.112	35.7285	32.6	1.1	35.86
10:20	32.19	1.113	35.8274	32.7	1.1	35.97
10:25	32.22	1.114	35.8930	32.5	1.1	35.75
10:30	32.21	1.114	35.8819	32.6	1.1	35.86
10:35	32.22	1.113	35.8608	32.5	1.1	35.75
10:40	32.27	1.115	35.9810	32.8	1.1	36.08
10:45	32.29	1.115	36.0033	32.9	1.1	36.19
10:50	32.28	1.114	35.9599	32.8	1.11	36.40
10:55	32.18	1.112	35.7841	32.6	1.1	35.86
11:00	32.1	1.11	35.631	32.4	1.1	35.64
11:05	32.1	1.112	35.6952	32.4	1.1	35.64
11:10	32.13	1.112	35.7285	32.6	1.1	35.86
11:15	32.14	1.112	35.7396	32.7	1.1	35.97
11:20	32.01	1.111	35.5631	32	1.1	35.2
11:25	31.39	1.1	34.529	32.2	1.1	35.42
11:30	31.74	1.105	35.0727	32	1.1	35.2
11:35	31.73	1.106	35.0933	32.1	1.1	35.31
11:40	31.77	1.107	35.1693	32.2	1.1	35.42
11:45	31.72	1.105	35.0506	32.1	1.1	35.31
11:50	31.84	1.108	35.2787	32.5	1.1	35.75
11:55	31.89	1.108	35.3341	32.6	1.1	35.86
12:00	31.8	1.105	35.139	32.8	1.1	36.08
12:05	31.72	1.103	34.9871	32.5	1.1	35.75
12:10	31.68	1.102	34.9113	32.5	1.1	35.75
12:15	31.66	1.102	34.8893	32.5	1.1	35.75
12:20	31.74	1.104	35.0409	32.4	1.1	35.64



Hour	fixed panel			mobile panel		
	Voltage	Current	Power	Voltage	Current	Power
12:25	31.66	1.103	34.9209	32.2	1.1	35.42
12:30	31.68	1.103	34.9430	32.4	1.1	35.64
12:35	32.15	1.112	35.7508	33.2	1.11	36.85
12:40	31.96	1.109	35.4436	33	1.1	36.3
12:45	31.74	1.106	35.1044	32.6	1.1	35.86
12:50	31.78	1.107	35.1804	32.8	1.1	36.08
12:55	31.7	1.106	35.0602	32.8	1.1	36.08
13:00	31.51	1.096	34.5349	32.3	1.1	35.53
13:05	30.1	1.084	32.6284	32	1.09	34.88
13:10	31.1	1.083	33.6813	31.09	1.09	33.88
13:15	30.85	1.084	33.4414	32.2	1.09	35.09
13:20	30.86	1.087	33.5448	32.2	1.1	35.42
13:25	29.72	1.084	32.2164	31.08	1.09	33.88
13:30	30.51	1.081	32.9813	31.8	1.09	34.66
13:35	30.69	1.083	33.2372	31.8	1.09	34.66
13:40	30.56	1.085	33.1576	32	1.09	34.88
13:45	30.95	1.087	33.6426	32.6	1.1	35.86
13:50	30.18	1.088	32.8358	32.2	1.1	35.42
13:55	29.68	1.085	32.2028	31.9	1.09	34.77
14:00	30.59	1.082	33.0983	31.9	1.09	34.77
14:05	30.75	1.083	33.3022	31.09	1.09	33.89
14:10	30.68	1.083	33.2264	32.5	1.1	35.75
14:15	30.76	1.086	33.4053	32.4	1.1	35.64
14:20	30.75	1.084	33.333	32.2	1.1	35.42
14:25	30.74	1.085	33.3529	32.6	1.1	35.86
14:30	30.73	1.084	33.3113	32.4	1.1	35.64
14:35	30.7	1.07	32.849	32.5	1.1	35.75
14:40	30.69	1.064	32.6541	32.5	1.1	35.75
14:45	30.7	1.063	32.6341	32.4	1.1	35.64
14:50	30.5	1.061	32.3605	32.3	1.09	35.20
14:55	30.7	1.063	32.6341	32.3	1.09	35.21
15:00	30.58	1.061	32.4453	32.4	1.1	35.64
15:05	30.66	1.061	32.5302	32.4	1.1	35.64
15:10	30.45	1.077	32.7946	32.3	1.1	35.53
15:15	30.53	1.063	32.4533	32.5	1.1	35.75
15:20	12.77	0.726	9.27102	10.5	0.66	6.93
15:25	31.09	1.069	33.2352	33.2	1.11	36.85
15:30	30.95	1.065	32.9617	33.1	1.11	36.74
15:35	6.59	0.588	3.87492	6.7	0.56	3.752
15:40	6.6	0.587	3.8742	7.9	0.6	4.74
15:45	31	1.091	33.821	34.6	1.13	39.09
15:50	6.6	0.547	3.6102	8.7	0.64	5.568
15:55	24.5	0.854	20.923	27.5	0.95	26.13
16:00	30.56	1.081	33.0353	34.9	1.14	39.78
16:05	29.56	1.062	31.3927	33.7	1.12	37.74
16:10	28.45	1.043	29.6733	33.1	1.11	36.74
16:15	27.62	1.029	28.4209	32.7	1.1	35.97
16:20	27.11	1.02	27.6522	32.7	1.1	35.97
16:25	26.11	1.002	26.1622	32.7	1.1	35.97
16:30	25.17	0.985	24.7924	32.7	1.1	35.97
16:35	24.01	0.963	23.1216	32.6	1.1	35.86
16:40	22.48	0.935	21.0188	32.6	1.1	35.86
16:45	19.91	0.887	17.6601	32.7	1.1	35.97
16:50	16.91	0.826	13.9676	32.3	1.09	35.20



Hour	fixed panel			mobile panel		
	Voltage	Current	Power	Voltage	Current	Power
16:55	16.69	0.822	3.71918	32.4	1.09	35.31
17:00	14.26	0.773	11.0229	32.2	1.09	35.09
17:05	12.11	0.727	8.80397	32.2	1.09	35.10
17:10	8.28	0.637	5.27436	32.1	1.09	34.98
17:15	1.1	0.233	0.2563	1.9	0.32	0.608
17:20	0.958	0.211	0.20213	1.6	0.29	0.464
17:25	0.869	0.195	0.16945	1.6	0.29	0.464
17:30	1.033	0.221	0.22829	1.28	0.69	0.883
17:35	0.684	0.16	0.10944	1.3	0.25	0.325
17:40	0.719	0.167	0.12007	26.1	0.91	23.75
17:45	0.551	0.131	0.07218	15.1	0.74	11.17
17:50	0.419	0.102	0.04273	0.6	0.13	0.078
17:55	0.333	0.08	0.02664	0.4	0.09	0.036
18:00	0.264	0.065	0.01716	0.3	0.07	0.021

Source: Authors, (2022).

Obtaining the graph of power generated for the first day with a fixed panel shown in figure 16.

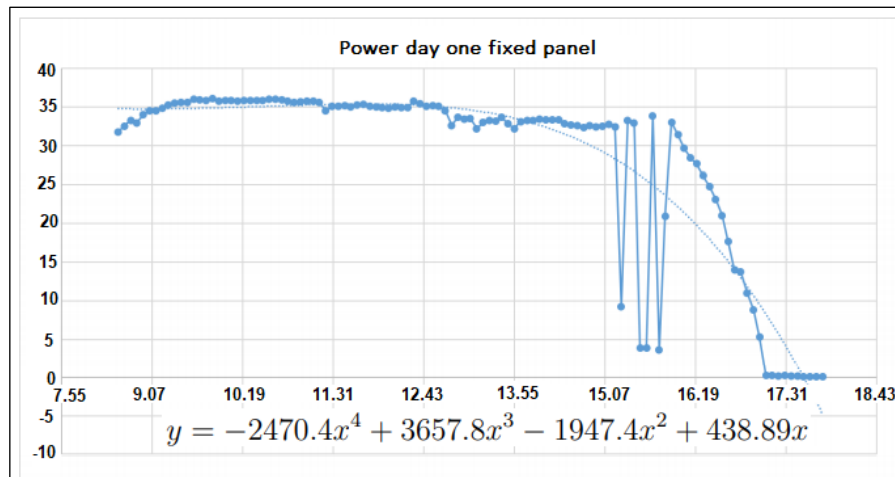


Figure 16: Graph of power generated first day with fixed panel.  
Source: Authors, (2022).

Obtaining the graph of power generated for the first day with a mobile panel shown in figure 17.

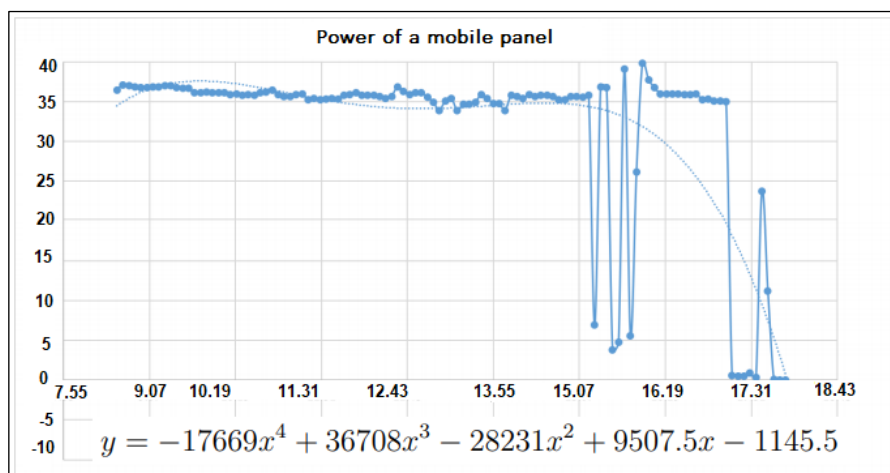


Figure 17: Graph of generated power, day one mobile panel  
Source: Authors, (2022).

With the measurements of the second day, the graph of power generated with a fixed panel is obtained, shown in figure 18.

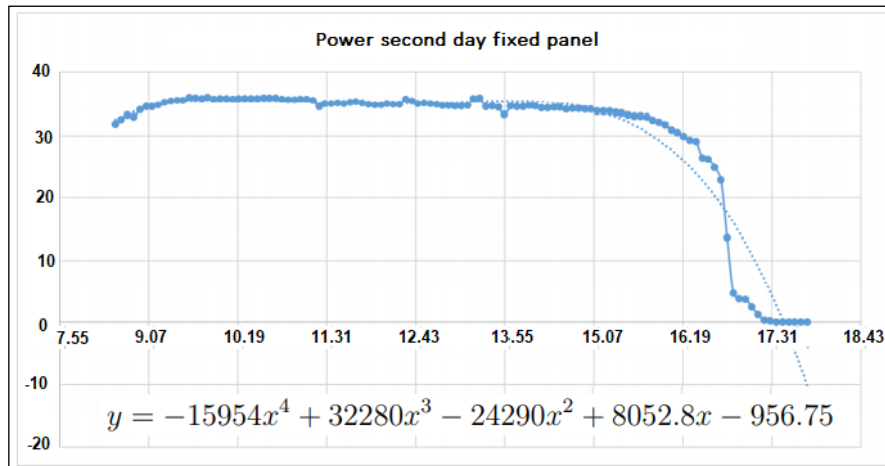


Figure 18: Graph of power generated second with fixed panel.  
Source: Authors, (2022).

With the measurements of the second day, the graph of power generated with the mobile panel is obtained, which is shown in figure 19.

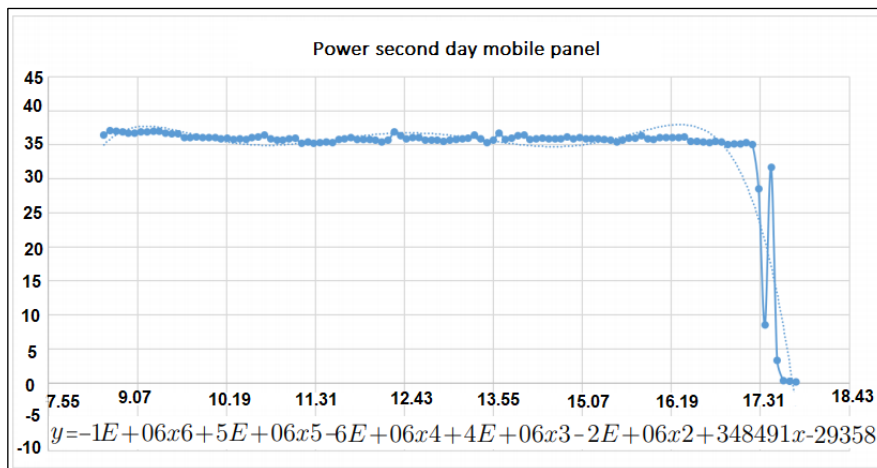


Figure 19: Graph of power generated second day with mobile panel.  
Source: Authors, (2022).

With the measurements of the third day, the graph of power generated with a fixed panel is obtained, which is shown in figure 20.

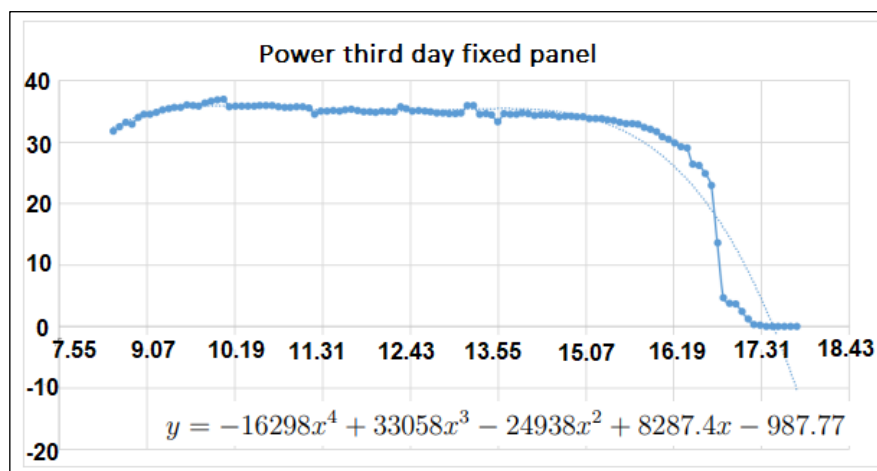


Figure 20: Graph of power generated third with fixed panel.  
Source: Authors, (2022).

With the measurements of the third day, the graph of power generated with the mobile panel is obtained, which is shown in figure 21.

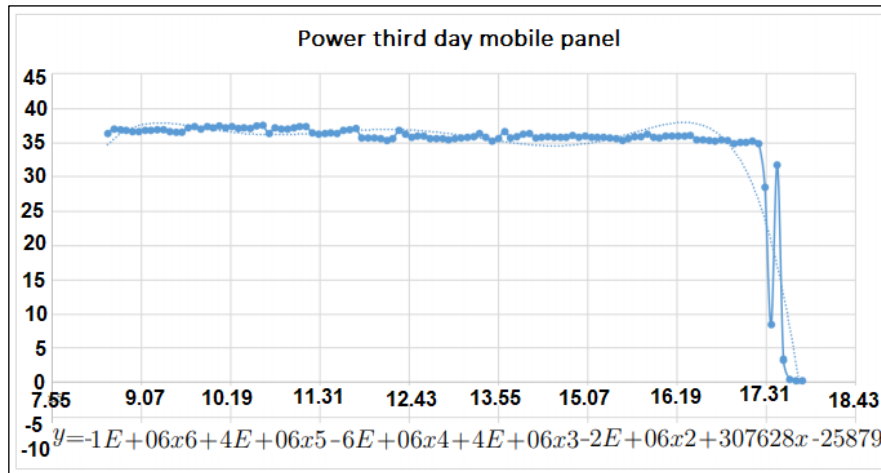


Figure 21: Graph of power generated third day with mobile panel.  
Source: Authors, (2022).

## VI. CONCLUSIONS

The built prototype complies with the required characteristics of tracking the sun on the polar axis from an initial position of the structure of 15o inclination on said axis and facing east for sunrise, by means of a fuzzy control system. which with respect to the classic controls is easier to understand the algorithm since it handles a linguistic programming method. To control the position of the panel with respect to the incidence of light, photoresistive elements were used, achieving a 40% increase in efficiency in solar panels with a mobile system with respect to fixed solar systems. The developed software allows maintaining the perpendicularity of the solar panel with respect to the incidence of solar rays, which is demonstrated with the data collected during the testing stage. The tests of the fixed system and the mobile system controlled by fuzzy control were carried out simultaneously, so the comparison made in the data collected has a higher degree of sustainability, since they were carried out under the same climatic conditions. It was not possible to carry out an implementation of a two-axis solar tracker system due to certain movement limitations in the structure and the short time in which the tests were carried out for the design used. The program used is designed to function exclusively for the structure used, however it is easily adjustable to a different structure that has a similar system.

## VII. AUTHOR'S CONTRIBUTION

**Conceptualization:** Omar Beltrán González, Jesús Hernández Aguilar, Francisco Eneldo López Monteagudo and Rafael Villela Varela.

**Methodology:** Omar Beltrán González, Jesús Hernández Aguilar, Francisco Eneldo López Monteagudo and Rafael Villela Varela

**Investigation:** Omar Beltrán González, Jesús Hernández Aguilar, Francisco Eneldo López Monteagudo, Rafael Villela Varela, Aurelio Beltrán Telles and Claudia Reyes Rivas.

**Discussion of results:** Omar Beltrán González, Jesús Hernández Aguilar, Francisco Eneldo López Monteagudo, Rafael Villela Varela, Aurelio Beltrán Telles and Claudia Reyes Rivas.

**Writing – Original Draft:** Omar Beltrán González and Jesús Hernández Aguilar

**Writing – Review and Editing:** Omar Beltrán González, Jesús Hernández Aguilar, Francisco Eneldo López Monteagudo and Rafael Villela Varela.

**Resources:** Omar Beltrán González and Jesús Hernández Aguilar, Francisco Eneldo López Monteagudo and Rafael Villela Varela.

**Supervision:** Francisco Eneldo López Monteagudo and Rafael Villela Varela.

**Approval of the final text:** Omar Beltrán González, Jesús Hernández Aguilar, Francisco Eneldo López Monteagudo and Rafael Villela Varela.

## VIII. ACKNOWLEDGMENTS

We thank the Autonomous University of Zacatecas and the Zacatecano council of science and technology for the support for the realization of this article.

## IX. REFERENCES

- [1] H. M. F. da Silva e F. J. C. Araújo, "Energia solar fotovoltaica no brasil: uma revisão bibliográfica", rease, vol. 8, n° 3, p. 859–869, mar. 2022.
- [2] M. Quijano and G. González, "Study of the Penetration of Photovoltaic Energy at the Self-consumption Customer Level using the IEEE 13-Node Test Feeder adapted to Panama," 2022 IEEE 40th Central America and Panama Convention (CONCAPAN), Panama, Panama, 2022, pp. 1-5, doi: 10.1109/CONCAPAN48024.2022.9997607.
- [3] J. N. Maciel, J. Javier Giménez Ledesma and O. Hideo Ando Junior, "Forecasting Solar Power Output Generation: A Systematic Review with the Proknow-C," in IEEE Latin America Transactions, vol. 19, no. 4, pp. 612-624, April 2021, doi: 10.1109/TLA.2021.9448544.
- [4] L. H. Vera, M. Cáceres, A. Firman, R. Gonzales Mayans and A. Busso, "Diseño y simulación de microrred híbrida aislada," 2022 IEEE Biennial Congress of Argentina (ARGENCON), San Juan, Argentina, 2022, pp. 1-7, doi: 10.1109/ARGENCON55245.2022.9939734.
- [5] F. R. Riccio Anastacio, Seguidor solar a dos ejes cuya posición se calcula utilizando los ángulos de elevación y Azimut del sol en Guayaquil, RECIMUNDO, vol. 6, n.º 1, pp. 225-231, feb. 2022.
- [6] E. Chacón-Pinzón, D. Arenas, y B. J. Parra, «Revisión del estado actual de los Sistemas de Energía Fotovoltaica», rinte, vol. 11, jul. 2021.
- [7] J. M. Rey et al., "A Review of Microgrids in Latin America: Laboratories and Test Systems," in IEEE Latin America Transactions, vol. 20, no. 6, pp. 1000-1011, June 2022, doi: 10.1109/TLA.2022.9757743.

- [8] A. -H. I. Mourad, H. Shareef, N. Ameen, A. H. Alhammadi, M. Iratni and A. S. Alkaabi, "A state-of-the-art review: Solar trackers," 2022 Advances in Science and Engineering Technology International Conferences (ASET), Dubai, United Arab Emirates, 2022, pp. 1-5, doi: 10.1109/ASET53988.2022.9735074.
- [9] A.Z. Hafez, A.M. Yousef, N.M. Harag, "Solar tracking systems: Technologies and trackers drive types – A review, Renewable and Sustainable Energy Reviews", Volume 91, 2018, Pages 754-782, ISSN 1364-0321, <https://doi.org/10.1016/j.rser.2018.03.094>.
- [10] A. Bahrami, C. Onyeka Okoye, "The performance and ranking pattern of PV systems incorporated with solar trackers in the northern hemisphere, Renewable and Sustainable Energy Reviews", Volume 97, 2018, Pages 138-151, ISSN 1364-0321, <https://doi.org/10.1016/j.rser.2018.08.035>.
- [11] A. -T. Nguyen, T. Taniguchi, L. Eciolaza, V. Campos, R. Palhares and M. Sugeno, "Fuzzy Control Systems: Past, Present and Future," in IEEE Computational Intelligence Magazine, vol. 14, no. 1, pp. 56-68, Feb. 2019, doi: 10.1109/MCI.2018.2881644.
- [12] Y. Hong, Hans J. Pasma, N. Quddus, M. Sam Mannan, "Supporting risk management decision making by converting linguistic graded qualitative risk matrices through interval type-2 fuzzy sets, Process Safety and Environmental Protection", Volume 134, 2020, Pages 308-322, ISSN 0957-5820, <https://doi.org/10.1016/j.psep.2019.12.001>.
- [13] O. Beltrán González, and J. Hernández Aguilar, "Design of a control system for a solar tracker implementing fuzzy logic in arduino", Bachelor's thesis, Electrical Engineering Academic Unit Autonomous University of Zacatecas, Mexico 2015.